

Measurement of Energy Loss in the ADS FFAG Foil

Chris Rogers

1 Data Taking

The principle of the experiment is to measure the synchronous phase of the beam as a function of RF voltage. When energy is "just" returned to the beam, the synchronous phase should be 90° .

A first dataset was taken on the afternoon of Friday 4th April, 2014. During that data taking the ion source was not performing well. Subsequent to the data taking the foil was found to have torn.

A second dataset was taken on the afternoon of Tuesday 24th June, 2014. The orbital frequency was measured as 1.577 MHz and this was used as the RF frequency. The beam could not be injected over $6.6 \mu\text{s}$ as this caused saturation in the beam loss monitors so a shorter injection period was used (*what period?*).

Due to the problems with the first dataset, that data is not studied in this analysis. Instead only the data taking during the June running is considered.

2 Input Signals

The analysis followed several stages. The time of the peaks in the RF signal and the bunch monitor signal S12 was calculated. The peak to peak time difference was studied in each signal to understand the stability of the signal and then used to calculate RF frequency. The time difference between adjacent peaks of the two signals was then studied to identify beam capture behaviour. The peak to peak voltage difference on the RF signal was used to calculate the RF voltage. The RF voltage was compared with the difference between time of RF signal and beam signal, and the resulting relationship was used to infer an energy loss.

10^6 counts were read out, with time between counts of 0.2 ns. The data was recorded by averaging over 128 ion source pulses.

2.1 Beam Monitor DC Signal

The beam monitor measures the wall current induced by the passage of the beam. The beam monitor acts as a capacitor; the wall current leads to a build up of charge on the beam monitor, creating an induced voltage. By measuring this induced voltage we get a measurement like

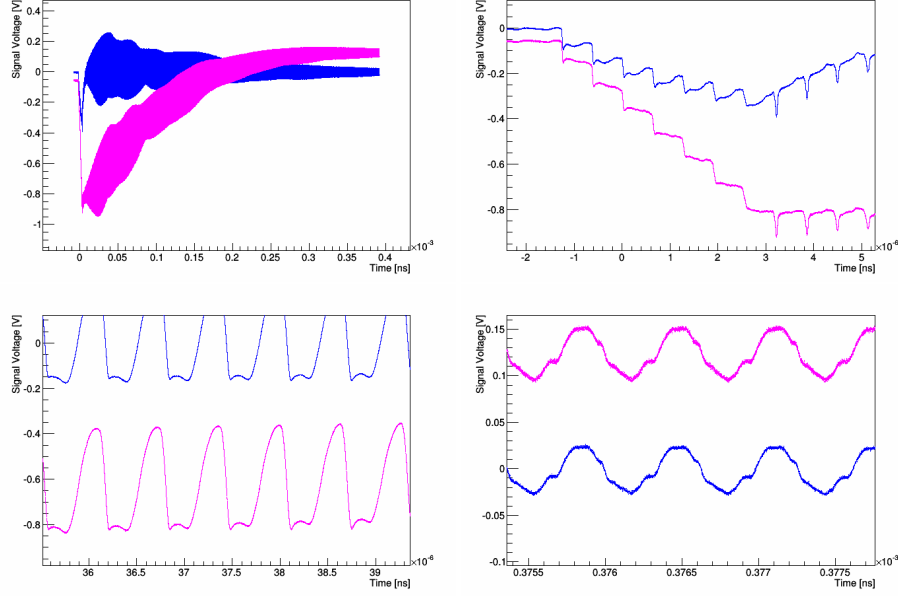


Fig. 1: Example of measured DC (pink) and AC (blue) signals. From top to bottom: full signal; signals around injection; signals in the middle of the cycle; signals at the end of the cycle. Note a negative signal corresponds to a positive current.

$$\int I/RCdt \quad (1)$$

what is the time constant?

2.2 Beam Monitor AC Signal

The "DC" signal is passed through a high-pass filter so that only the high-frequency part of the "DC" signal i.e. the changes in the DC signal are read out. This is called the beam monitor "AC" signal. *rogers guess*

2.3 RF Signal

The RF signal was generated by means of a pick-up in the RF cavity.

2.4 Example signals

A sample set of signals is shown in Fig. 1. Near to injection the DC component of the signal is observed to be reduced in the AC signal.

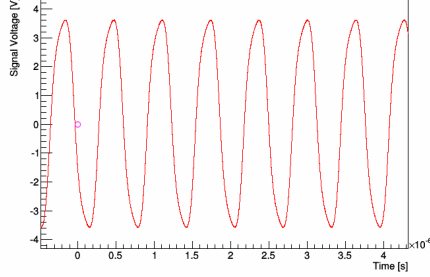


Fig. 2: Example of measured RF signal.

A false peak is observed around injection in the AC signal, and it is thought that this is an artefact of the filtering electronics. *really?*

In the middle of the cycle the double peak is noted. This will be discussed later. At the end of the cycle, signal noise becomes significant.

A sample RF signal is shown in Fig. 2. It is noted that the RF signal is not a precise sinusoid. *Is this a feature of the electronics? Is the cavity Q low enough for that?*

3 Measurement of Bunch Phase

The algorithm used to find the bunch phase relative to the RF cavity is next described.

3.1 Peak Finding Algorithm

Peaks were found in the first instance by smoothing the data using a Gaussian function with standard deviation 50 ns. This was followed by a search for peaks performed by looking for the peak values within a 50 ns window. The window was advanced in steps of 25 ns and the peak value was recorded within the window. Peak values at the window edge were ignored. Where multiple peaks were found with this algorithm, they were recorded.

This initial estimate was refined by fitting a quadratic function to the raw (unsmoothed) data points in the region of the peak. The points used for fitting were dynamically selected by requiring that the residuals of the fit $x(\text{fit}) - x(\text{data})$ within some window should not have a standard deviation much larger than the estimated standard deviation of the data very close to the peak. The window was made smaller until this condition was met. The time and magnitude of the peak, t_p, y_p were estimated from the fit parameters, according to

$$y = a_0 + a_1 t + a_2 t^2 \quad (2)$$

$$t_p = -\frac{a_1}{2a_2} \quad (3)$$

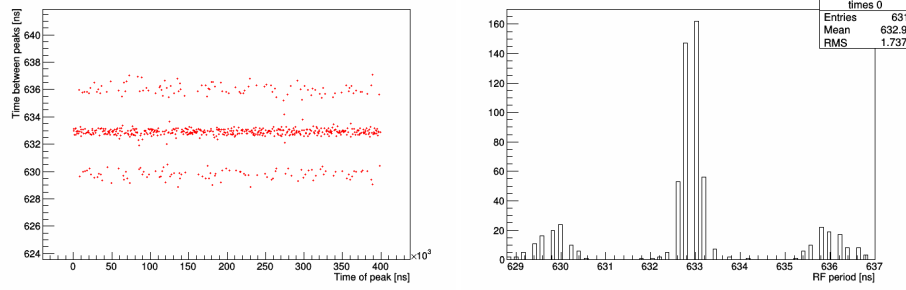


Fig. 3: Distribution of time between adjacent RF peaks (top) as a function of time (bottom) projection of top histogram. The 0.2 ns arises from the peak finding algorithm. Side bands are visible 3 ns from the main peak; the source is not known.

$$y_p = -\frac{a_1^2}{4a_2} + a_0 \quad (4)$$

The errors were calculated using the standard relationship

$$\mathbf{V}(t_p, y_p) = \mathbf{J}\mathbf{V}(\vec{a})\mathbf{J}^T \quad (5)$$

where \mathbf{V} are the covariance matrices. $\mathbf{V}(\vec{a})$ was calculated by taking the numerical derivative of the fit parameters with respect to the χ^2 , which is done automatically by the ROOT software used for fitting. \mathbf{J} is the Jacobian for $(t_p(\vec{a}), y_p(\vec{a}))$, given by

$$\mathbf{J} = \begin{pmatrix} 0 & -1/2a_2 & a_1/2a_2^2 \\ 1 & -a_1/2a_2 & a_1^2/4a_2^2 \end{pmatrix} \quad (6)$$

3.2 RF Signal Peaks

The magnitude and time of peaks and troughs was calculated using the peak finding algorithm outlined above. The time difference between adjacent peaks is shown in Fig. 3, both as a function of time and in projection. The 0.2 ns divisions are a consequence of the peak finding algorithm. The peak finding algorithm can be made more accurate (but it probably doesn't really matter).

The frequency is seen to be stable across many pulses, to within the measurement error. There appear to be side-bands a few ns away from the main peak and this is also observed for other samples. To give an order of magnitude for the significance of these features, it is noted that simulation through the field map with $F = 810A$ and $D = 1020A$

$$dT/dE = 23.07ns/MeV \quad (7)$$

Could check for this feature with FFT - just in case it is the fitting algorithm doing it.

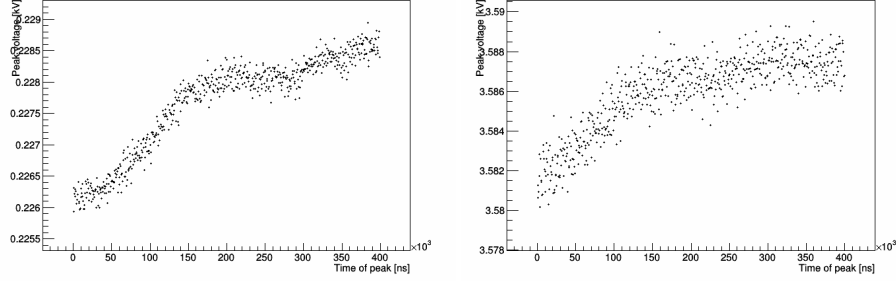


Fig. 4: Peak voltage (top) for 0.229 V and (bottom) for 3.589 V signals. The dogleg feature is noted, where the RF voltage takes some time to come up to a flat top.

The mean RF period is measured as 632.9 ± 0.1 ns. The RF frequency is consistent at different voltages.

The RF voltage is taken as half the peak to trough distance. The RF voltage as a function of time within the sample is shown in Fig. ???. The dogleg feature is noted. The absolute magnitude of the "dogleg" varies between 0.002 and 0.008 V, the fractional magnitude staying less than around 1 %. The width of the peak spread is consistent with errors reported by the peak fitting algorithm.

The average RF voltages (half peak to trough for each sample) are listed below:

- 0.101
- 0.16
- 0.229
- 0.308
- 0.406
- 0.523
- 0.664
- 0.835
- 1.023
- 1.241
- 1.504
- 1.792
- 2.106

- 2.318
- 2.545
- 2.692
- 2.876
- 3.057
- 3.232
- 3.407
- 3.589

3.3 Bunch Monitor Signal

For higher RF voltages, the beam is well captured and the peak-to-peak period is roughly constant across a reasonable range. For lower voltages the beam is less well captured and the peak-to-peak period shows much greater variation. Even for the case where the beam is well captured, the spread in peak-to-peak times is larger than the calculated error in the peak finder, indicating that there may be some debunching or other behaviour occurring.

Bunch monitor signals for a selection of the measured data sets are shown in Fig. 5. Further interpretation of the bunch monitor signals is given by comparison to Monte Carlo in section 4.

3.4 Measured RF Phase of Captured Bunch

The phase of the measured peaks in the bunch monitor signal are used to calculate the RF phase of the captured bunch.

The bunch phase is calculated using the distance between the RF peak and the bunch peak after the first 150 μs of the cycle. Before 150 μs there is significant filamentation as parts of the beam which are not captured are lost, so this region is excluded from the analysis.

The projection of the turn-by-turn measured phase is used to estimate the actual synchronous phase of the RF. The peak in the measured beam phase is found and the error on this measurement is taken to be the full-width of the peak at half maximum.

Where more than one peak is visible, if the alternate peaks have a magnitude more than half the size of the principle peak then the error on the measurement is taken to be the distance between the upper bound on the upper peak and the lower bound on the lower peak. This reflects uncertainty in the actual synchronous phase when the bunch is oscillating, for example in the higher voltage cases.

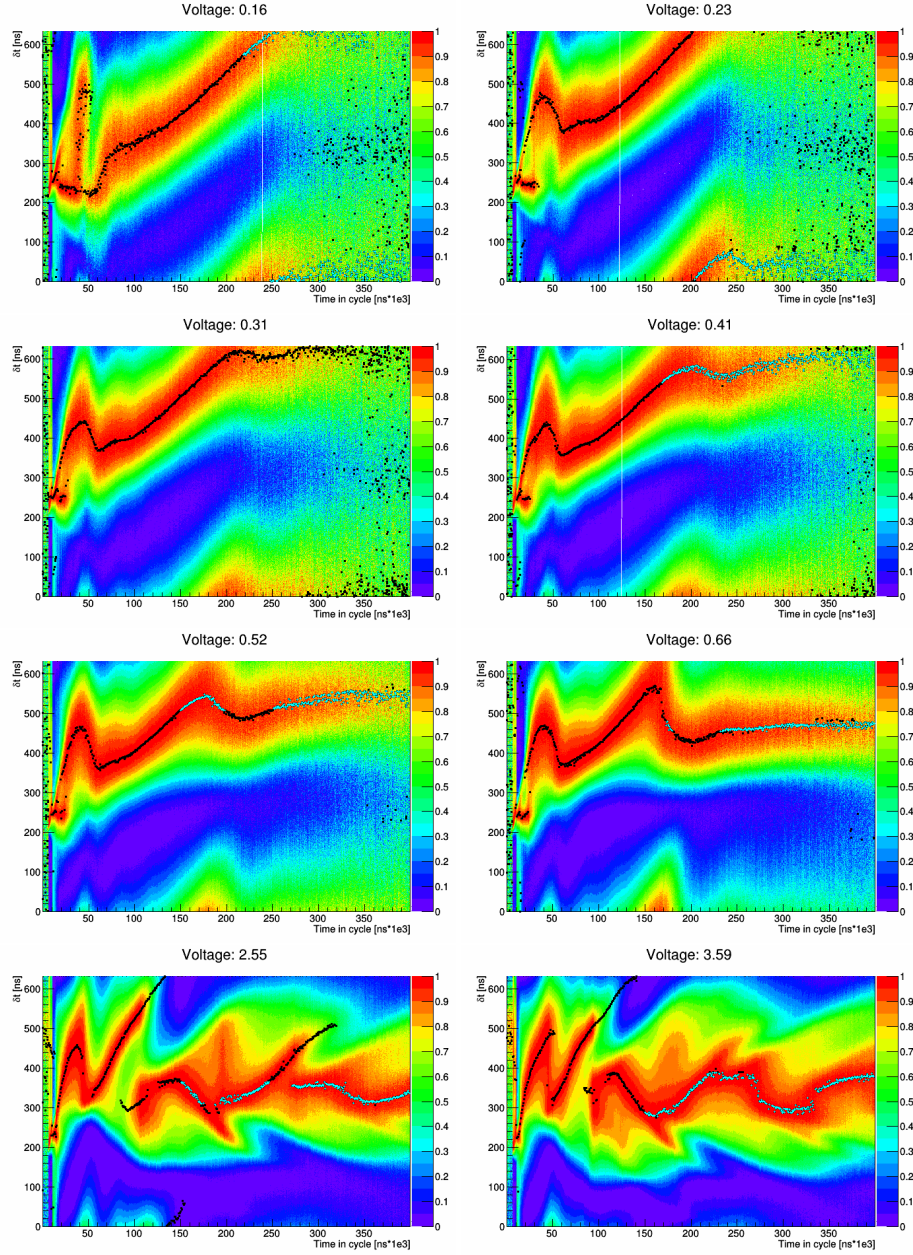


Fig. 5: BPM signal for RF voltages where the beam is not considered to be captured. The colours show AC signal voltage. δt is the time relative to the most recent RF peak. The signal is normalised in to lie within the range (0, 1) on each successive RF period. The points show the position of the measured peaks in the beam current. Blue points were included in the RF phase analysis and black points were excluded.

3.5 Measured Voltage Threshold

The measured phase of the bunch for different RF voltages is shown in fig. 6.

In order to calculate a measured thickness of the foil, the RF phase is compared to the peak voltage. When the beam is coasting, the energy returned to the beam should balance the energy lost on the foil. Hence

$$V_0 = c\delta W \sin(\phi_s + d\phi). \quad (8)$$

where V_0 is the peak voltage, c is a calibration constant that scales the pickup voltage to the voltage experienced by a proton in the FFAG, δW is the energy lost on the foil, ϕ_s is the reference phase and $d\phi$ is a calibration constant representing azimuthal offset of the RF cavity and the bunch monitor, cable lengths and any associated electronics signal delays.

The calibration constant c has value $1e3$ *with what errors*.

By inspection of Fig. 5, the beam at 0.23 V is not captured as there is no region where the beam has a constant phase before it is lost. The beam at 0.66 V certainly is captured as there is a clear region where the RF phase is constant.

Based on this analysis, the voltage required to generate an RF bucket is considered to be in the range 0.23 kV to 0.66 kV.

It is possible to use the measured phase of the beam to better constrain the energy loss due to the foil. The phase of the beam relative to the RF can be calculated using the peaks shown in 5.

The quality of fit, when synchronous phase is included, is shown in Fig. 6. Minuit was used to fit equation 8, minimising $\sum \chi^2$. Several fitting attempts were made, in each case constraining the fitting routine to find a voltage below some minimum value, and including only data with voltages above this minimum value.

The results of the fit and the $\sum \chi^2$ are shown in in Table 1. Based on this analysis, the phase of the bunch is not consistent with the model for voltages below 0.52 V. The minimum RF voltage required to bunch the beam is measured to be at least 0.41 kV.

3.6 Measured Thickness

The measured energy lost in the foil is compared with the Bethe-Bloch model [?] and the GEANT4 QGSP energy loss model [?] to deduce a measured foil thickness. The design thickness is 20 [μ g/cm²] *was it 10 or 20?*.

4 Comparison to Monte Carlo

A beam was simulated in the FFAG. Particles were thrown with initial time distributed randomly over a given time interval (0, 6400) ns and with no energy spread. The particle positions, momenta and times were subsequently recorded each time they were simulated crossing an output plane (i.e. once per turn). Unless specified stochastic processes are disabled - the particles only experience mean energy loss and no scattering.

Lowest voltage setting [V]	Fitted voltage [V]	Fitted phase [rad]	Degrees of freedom	$\sum \chi^2$	Probability
0.16004	0.12316	-4.08641	20.0	406.1685	0.0
0.22874	0.22462	-3.96561	19.0	192.54915	0.0
0.30771	0.29869	-3.82594	18.0	114.25484	0.0
0.40573	0.40542	-3.62116	17.0	51.86977	0.0
0.52289	0.53894	-3.43218	16.0	36.29481	0.0
0.66366	0.51166	-3.44335	15.0	22.21081	0.1
0.8353	0.64442	-3.25901	14.0	8.94221	0.83
1.02319	0.93069	-3.0	13.0	3.01842	1.0
1.24096	0.7548	-3.11346	12.0	3.27581	0.99
1.50383	0.89299	-3.04173	11.0	2.89378	0.99

Tab. 1: Fitted RF voltage and phase for different sets of minimum allowed voltage.

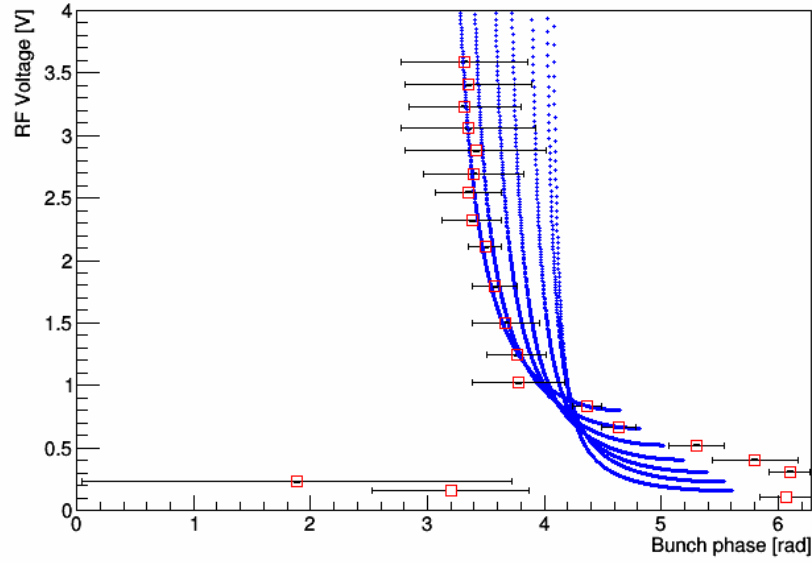
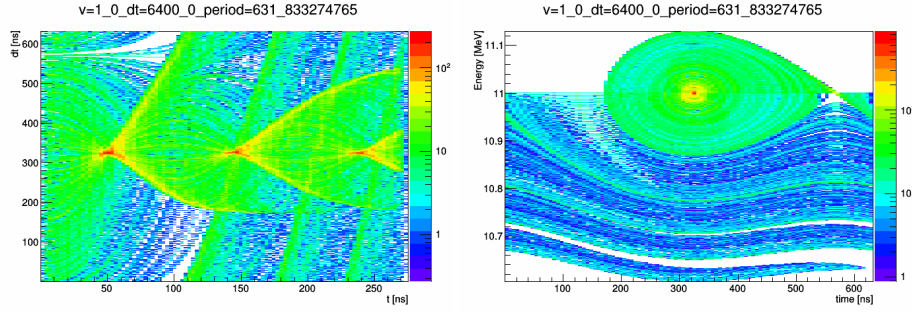


Fig. 6: Measured synchronous phase relative compared to RF peak voltage. Fit curves are shown including various threshold voltages.

	Bethe Bloch	Geant4.9.6p02 QGSP model
Mean stopping power	37.6 MeV cm ² g	34.0 MeV cm ² g
By inspection	6.11 - 17.6 μ g/cm ²	6.76 - 19.4 μ g/cm ²
Fit	> 10.9 μ g/cm ²	> 12.1 μ g/cm ²
Combined	10.9 - 17.6 μ g/cm ²	12.1 - 19.4 μ g/cm ²

Tab. 2: Model stopping power and corresponding foil thicknesses.

Fig. 7: Monte Carlo simulation of a nominal bunch. (Left) number of particles passing through the output plane in a given time bin (Right) Total time vs energy for a nominal bunch. The units for the abscissa are $1e3ns$.

A sample simulated data set is shown in Fig. 7. The beam has initially no energy spread and fills the RF period completely (100 % phase spread). In time, the bunch can be seen to be compressed by the RF focussing with a focussing period of about $100 \mu s$. Some filamentation is observed of the beam that is not caught in the RF bucket.

4.1 Sensitivity to RF Voltage

4.2 Sensitivity to Injection Interval

During this study, the beam was injected over several turns. If the beam injection is not an integer number of turns, there will be a fractional surplus during part of the turn. One may speculate that this causes a bunch-like feature in the longitudinal distribution.

The ring was simulated with an injection interval of 6 turns and 6.5 turns, as shown in Fig. 8. No effects are visible on the beam due to the variable injection interval.

4.3 Sensitivity to Stochastic Processes

The effect of stochastic processes on the beam can be seen in Fig. 9. The behaviour of the beam longitudinally looks similar; there is now significant

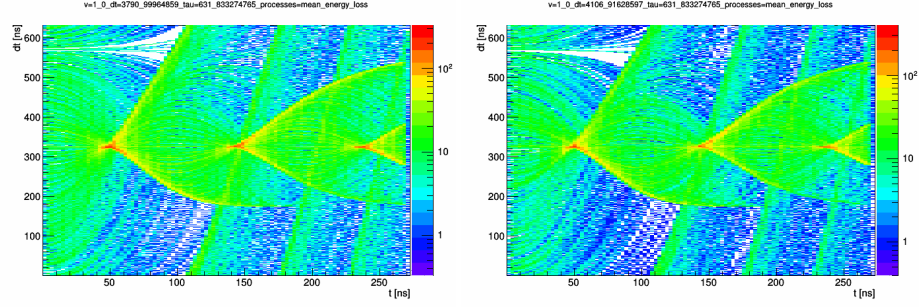


Fig. 8: Simulation with variable injection interval (left) injection interval 6 turns (right) injection interval 6.5 turns. The units for the abscissa are $1e3ns$.

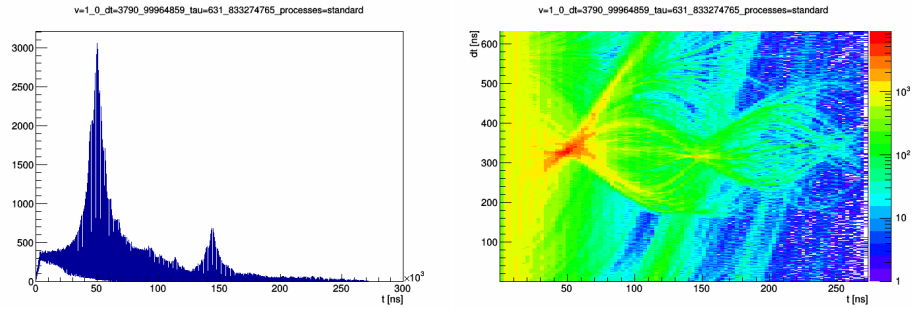


Fig. 9: Simulation with all GEANT4 QGSP physics processes enabled: (left) number of muons crossing an output plane in a time step, as a function of time; (right) number of muons crossing an output plane in a time step, as a function of time and phase. The units for the abscissa are $1e3ns$.

beam loss during the cycle, which is thought to be caused by protons scattering vertically until the foil holder is hit.

4.4 Sensitivity to RF Frequency

4.5 Sensitivity to Energy Spread

5 Discussion